Title

Early events in the fibrillation of monomeric insulin.

Journal

Journal of Biological Chemistry, 280(52)

ISSN

0021-9258

Authors

Ahmad, Atta
Uversky, Vladimir N
Hong, Dongpyo
et al.

Publication Date

2005-12-30

Peer reviewed

Early events in the fibrillation of monomeric insulin†

†This research was supported in part by a grant from UC BioSTAR and Novo Nordisk A/S to ALF

*Atta Ahmad, Vladimir N. Uversky, Dongpyo Hong and Anthony L. Fink**

Department of Chemistry and Biochemistry, University of California, Santa Cruz, California 95064, USA

AUTHOR EMAIL ADDRESS: fink@chemistry.ucsc.edu

RECEIVED DATE:

TITLE RUNNING HEAD: Early stages of insulin fibrillation

CORRESPONDING AUTHOR FOOTNOTE: *To whom correspondence should be addressed: Department of Chemistry and Biochemistry, University of California, Santa Cruz, California 95064, USA. Telephone: (831) 459-2744. Fax: (831) 459-2935. E-mail address: enzyme@ucsc.edu

ABSTRACT.

Insulin has a largely α-helical structure, and exists as a mixture of hexameric, dimeric and monomeric states in solution, depending on the conditions: the protein is p monomeric in 20% acetic acid. Insulin forms amyloid-like fibrils under a variety of conditions, especially at low pH. In this study we investigated the fibrillation of monomeric human insulin by monitoring changes in CD, ATR-FTIR, ANS fluorescence, ThT fluorescence, dynamic light scattering and H/D exchange during the early stages of the fibrillation process in order to provide insight into early events involving the monomer. The results demonstrate the existence of structural changes occurring before the onset of fibril formation, which are detectable by multiple probes. The data indicate at least two major populations of intermediates between the native monomer and fibrils. Both have significantly non-native conformations, and indicate that fibrillation occurs from a beta-rich structure significantly distinct from the native fold.

KEYWORDS: Insulin; Aggregation; Fibrils; Partially folded intermediate; Oligomers; Self-association

ABBREVIATIONS: CD, circular dichroism; FTIR, Fourier transform infrared; ThT, thioflavin T; ANS, 8-anilino naphthalene sulfonic acid; DLS, dynamic light scattering.

INTRODUCTION

A number of human diseases have been found to be caused by the pathogenic deposition of proteins in the form of amyloid-like fibrils (*1-7*). Several non-pathogenic proteins and peptides have also been found to undergo amyloid like fibril formation on destabilization of their native state (*7-10*). The fact that structurally and sequentially non-homologous proteins are able to self-assemble into fibrils possessing similar morphology (e. g. 10-18 nm width, birefringence to polarized light, and cross-beta structure) suggests a common molecular mechanism in the fibrillation pathways. A variety of hypotheses for the mechanism of fibril formation have been proposed.

Insulin is a 51-residue hormone with a largely α-helical structure. It exists as a mixture of hexameric, dimeric and monomeric states in solution, with the relative population of different oligomeric species being strongly dependent on the environmental conditions: the protein is predominantly monomeric in 20% acetic acid, dimeric in 20 mM HCl and is hexameric at pH 7.5 in the presence of zinc. Insulin forms amyloid-like fibrils under a variety of conditions (*11-13*), with various overall morphologies depending on the arrangement of constituent protofilaments (*14;15*). Insulin fibrils pose a variety of problems in biomedical and biotechnological applications. Amyloid deposits of insulin have been observed in patients with diabetes after repeated injection and in normal ageing, as well as after subcutaneous insulin infusion and (*16;17*).

In our previous work we have shown the important role of partially folded intermediates in insulin fibrillation *in vitro* (*13;18-20*). In fact, our studies showed that insulin, which is a hexamer at physiological pH, undergoes rapid fibrillation starting at relatively low concentrations of Gdn.HCl and urea. The predominant species characterized by various biophysical techniques under these conditions was shown to be a partially folded, expanded

monomer, which is present in solutions containing up to 6 M Gdn.HCl or 8 M urea (*18;19*). Furthermore, the dissociation of the hexamer under these conditions was found to be the major rate-limiting step. Interestingly, in the presence of 20% acetic acid; i.e., under the conditions where insulin exists as a native monomer, the addition of Gdn.HCl was shown to result in the formation of a partially folded expanded conformation with high propensity to fibrillate (*18*). However, the addition of urea under the same conditions slowed down the rate of fibrillation (approximately 5-fold at 0.75 M urea), which has been explained by the appearance of non-native conformation with significantly increased α-helical content compared to the native form of the protein (*19*). It was very interesting to observe the effective formation of fibrils even at high denaturant concentration where the protein exists in an extensively unfolded conformation (*18;19*). All these observations led us to assume that the pathway for insulin fibrillation can be described by a simple model hexamer → modified monomer → fibrils (*13;18-20*). The present paper, in conjunction with earlier studies on insulin fibrillation (*11-13;18-20*), provides further evidence for the relationship between the conformational changes and the propensity of insulin to fibrillate. To this end the changes in biophysical properties (detected by CD, ATR-FTIR, dynamic light scattering, ANS fluorescence and H/D exchange mass spectrometry) accompanying the fibrillation of monomeric insulin (monitored by ThT fluorescence) have been analyzed as a function of time to provide insight of the very early events taking place in the monomer before it undergoes fibril formation. The results demonstrate the existence of significant structural changes occurring in monomeric insulin before the onset of fibril formation, which correspond to at least two major populations of intermediates. Both have significantly non-native conformations, and indicate that fibrillation occurs from a beta-rich structure significantly distinct from the native fold.

EXPERIMENTAL PROCEDURES

Materials - Human insulin with zinc was kindly provided by Novo Nordisk, Copenhagen, Denmark. All the chemicals were analytical grade, and were from EM Sciences or Sigma. Thioflavin T was obtained from Fluka.

Preparation of samples - Solutions of monomeric human insulin, 2 and 4 mg/ml, were freshly prepared in 20% acetic acid. The concentration of insulin was determined using an extinction coefficient of 1.0 for 1 mg/ml at 276 nm (*14*). Stock (1 mM) solutions of Thioflavin T were prepared by dissolving ThT in double distilled water and the concentration determined using a molar extinction coefficient of 24,420 M^{-1} cm^{-1} at 420 nm. ThT was stored at 4°C, protected from light.

Incubation of Insulin for fibrillation - 500 μL of insulin, 2 or 4 mg/ml in 20% acetic acid, was incubated at 37 °C in a glass vial on a stirrer with a small magnetic bead spinning at the bottom of the vial at approximately 600 rpm. Aliquots from this solution were taken at desired time intervals.

ThT assay for determining kinetics of fibrillation - Free ThT has excitation and emission maxima at ~350 and ~450 nm, respectively. However, upon binding to fibrils the excitation and emission λ_{max} change to ~450 and ~485 nm, respectively (*21;22*). 5 μL aliquots of sample were added to solution containing 20 μM ThT in 20 mM Tris-HCl buffer pH 7.4, shaken a few times before measuring the fluorescence emission on a FluoroMax-3 spectrofluorometer from Instruments S.A., Inc. Jobin Yvon-Spex, at room temperature. A background fluorescence spectra obtained by running a blank buffer was subtracted from each sample fluorescence spectra. The excitation wavelength was 444 nm and the emission recorded at 482 nm. Fluorescence intensity at 482 nm were plotted against time and the kinetic profiles were analyzed by curve fitting, using SigmaPlot software (*18*).

ANS Fluorescence - 5 μL aliquots from the incubated mixture were added to solutions containing 5 μM ANS in 20 mM Tris-HCl buffer pH 7.4 and the fluorescence measured with a FluoroMax-3 spectrofluorometer at room temperature. The excitation wavelength was 350 nm and the emission measured at 460 nm. The values of fluorescence intensity at 462 nm and the values of maximal wavelength of the emission spectra were plotted against time. The profiles were fitted using curve fitting with SigmaPlot.

Circular Dichroism - 40 μL of the aliquot were placed in a cuvette with 0.1 mM path length and CD spectra were collected on an AVIV 60DS circular dichroism spectrophotometer (Aviv Associates, Lakewood, NJ) at 25°C. A CD spectrum of the buffer was subtracted from the sample spectra for background correction. Spectra were recorded using a step size of 0.5 nm and a bandwidth of 1.5 nm. Phase diagrams were plotted as previously described (*18;19*).

Attenuated Total Reflectance Fourier Transform Infrared Spectroscopy (ATR-FTIR). FTIR spectra were recorded on a ThermoNicolet Nexus 670 FTIR spectrophotometer from 4000 to 400 cm^{-1} using a resolution of 2 cm^{-1} and an accumulation of 256 scans. 40 μL of the aliquot from the incubation mixture (4 mg/ml insulin at 37^{o}C with continuous stirring) was withdrawn at various intervals of time and spread uniformly on the surface of a germanium crystal using nitrogen to form a hydrated thin film. The system was continuously purged with dry nitrogen. Background and water vapor subtractions were performed until a straight baseline was obtained between 2000 and 1750 cm-1. Curve fitting of the amide I regions (raw spectra) was performed using GRAMS 32. Second derivative and Fourier self-deconvolved spectra were used as a peak position guide for the curve fitting procedure. The phase diagrams were plotted based on the extension of the concept described in the circular dichroism section above.

H/D exchange ESI MS Measurements. The mass spectra were recorded on a MICROMASS QUATTRO II mass spectrometer (Micromass, Altrimcham, U.K.) equipped with an electrospray

ionization ion source. The sample solution was introduced into the ion source using a Harvard Apparatus model 11 syringe pump. In order to improve the sensitivity and stability of the ion beam, the source was operated at 80°C. The electrospray capillary was set at 3.5 kV and the cone voltage at 20 V. Nitrogen was used as the nebulizing and drying gas at a flow rate of 15 and 300 L/h, respectively. The spectra were acquired and processed using MassLynx software supplied with the instrument. The mass spectrum was scanned from *m*/*z* 500 to 2200 in 6 s, and the spectra presented are averages of five spectra. The charge states were determined by MassLynx software, and the deconvolution of the spectra was carried out using MaxEnt software.

Stock insulin solution of 10 mg/ml was prepared in 20% acetic acid. Aliquots from this were added to obtain final concentration of 4 mg/ml insulin in 20% acetic acid with 5, 10 and 60% of D2O, respectively. The samples were incubated for 0, 6, 12 and 24 hours and diluted 100 times before injecting into the mass spectrometer.

Monitoring monomeric and oligomeric insulin by dynamic light scattering - DLS measurements were performed at 20 ^{o}C using a DynaPro (Wyatt Technology) model 99-E-50 instrument. Aliquots of 10 µL of the incubation solution (4 mg/ml insulin at 37 ^{o}C) were centrifuged before measuring DLS. 1 µL of the supernatant was diluted with 10 µL-filtered 20 % acetic acid buffer in the DLS cuvette, and measurements were taken within 3-7 min. Scattering peaks less than 0.1 nm radius and more than 1000 nm were ignored.

RESULTS

Changes in the conformation of insulin were monitored by a variety of probes during incubation of *monomeric* insulin under conditions leading to fibrillation. By starting with monomeric insulin complications due to associated states of native insulin (, such as the hexamer

or dimer), were avoided. The apparent pH of a 20% acetic acid solution is 1.8. Such low pHs are used in the commercial production of recombinant human insulin. Unless otherwise noted the experiments involved incubation of 4 mg/ml insulin in 20% acetic acid at 37°C with continuous agitation.

Fibril Formation monitored by ThT Fluorescence - Thioflavin T is a fluorescent dye that is frequently used as a specific probe for fibril formation *in vitro* (*21;22*). Changes in ThT emission at 482 nm as a function of time of insulin incubation in 20% acetic acid at 37 ^{o}C (i.e. conditions where insulin is known to be monomeric) with continuous shaking are shown in Figure 1. The figure indicates that the increase in ThT fluorescence intensity follows a typical sigmoidal pattern both at 2.0 and 4.0 mg/ml insulin. The initial region with no significant changes in fluorescence corresponds to the nucleation phase and the region showing rapid increase in fluorescence is the elongation phase, and the final plateau region is the maturation phase of fibrillation. Analysis of the ThT curves showed that the fibrillation of protein at 4.0 and 2.0 mg/ml is characterized by lag-times of 5.0 and 11.4 hrs, respectively. Thus at 2-fold higher protein concentrations the onset of fibrillation takes 2-fold shorter time than that at the lower concentration. The 2-fold higher fluorescence signal in the case of 4.0 mg/ml insulin solution also indicates a 2-fold higher quantity of fibrils.

ANS Fluorescence - ANS is able to bind to solvent-exposed hydrophobic regions of proteins and has been widely used for the characterization of the partially folded intermediates (*23-25*). The excitation λ_{max} of free dye is at 350 nm and emission λ_{max} is at 514 nm. On binding to solvent-exposed hydrophobic regions of proteins the emission λ_{max} changes to around 460 nm, accompanied by a dramatic enhancement in fluorescence intensity (*23-26*). The kinetic profile of ANS binding to insulin at 4 mg/mL incubated under the conditions described above is shown in Figure 2. At 0 hrs the emission intensity of ANS is very low with a maximum at 510 nm, which

is characteristic of free ANS. At 2.5 hrs of incubation a sharp increase in the fluorescence at 460 nm is observed, which is accompanied by a concomitant blue shift in emission λ_{max}. These changes indicate an increase in the efficiency of ANS binding to insulin, suggesting that the protein undergoes structural changes giving rise to the appearance of solvent-exposed hydrophobic regions under these conditions. Interestingly, the blue shift of maximal ANS fluorescence reached its maximum (~460 nm) after 6.0 hrs of incubation, whereas the increase in the ANS fluorescence intensity showed saturation only after 12.0 hrs (see Figure 2). This indicates that well before the formation of any ThT-detectable fibrils, insulin begins to undergo a series of sequential conformational changes, with transitions between 0 and 2.5; 2.5 and 6.0; and 6.0 and 12.0 hrs of incubation.

H/D Exchange Mass Spectrometry – Mass spectrometry has been used to measure H/D exchange of insulin (*27;28*): the results showed that insulin undergoes H/D exchange by both fast (EX1) and slow (EX2) mechanisms. In our studies, we treated insulin with different concentrations of D_2O in the presence of 20% acetic acid for different amounts of time as shown in Table 1. No H/D exchange was observed in 5% D_2O for as long as 24 hrs of incubation at 37 ^oC. In the presence of 10% D_2O a slow exchange process was observed with 20 protons exchanging after six hours of incubation. The exchange number did not change up to 24 hrs of incubation. However, 60% D_2O resulted in fast (EX_1) and slow (EX_2) exchange processes: 40 protons were found to exchange rapidly on addition of D_2O, and after incubation for 6 hours, 10 more protons were found to undergo exchange by a slow process. These data suggest that proton exchange in monomeric insulin is significantly dependent on D_2O concentration, and that prolonged incubation of the protein in high D_2O concentrations shows the presence of at least 10 buried protons.

To detect changes (if any) of these buried protons during the fibrillation process, aliquots of insulin (4.0 mg/ml, incubated at 37 ^{o}C with continuous stirring) were taken at regular intervals and then treated with the different concentrations of D_2O. Table 1 shows that the addition of 5% and 10% D_2O did not result in any exchange of insulin protons at any time point between 0-5 hrs of incubation. However, as expected, 40 protons exchanged at zero time with 60% D_2O. The number of exchangeable protons did not change for up to 2.0 hours of incubation. However, after incubation for 2.5 hours, the extra 10 protons were found to undergo exchange. These observations clearly show that the conformation of insulin is changed in such a way that the buried portion of the protein becomes exposed to the solvent at this point of incubation, presumably through formation of a partially folded intermediate.

ATR-FTIR Studies - Application of ATR FTIR to study the process of protein aggregation has been reviewed (*29;30*). Previous studies showed that monomeric insulin is characterized by a peak at 1654 cm^{-1} characteristic of α-helical proteins, and that on conversion into fibrils the peak shifts to 1628 cm^{-1}, consistent with the high β-structure content of the fibrils (*31-33*). Figure 3A shows ATR FTIR spectra of insulin measured at various intervals of incubation. Plots of absorbance against time of incubation (Figure 3B) show that only very small changes in the spectral shape and intensity take place for the first 2.5 hours of incubation. Two transitions involving significant increases in intensity at 1628 cm^{-1} (mirrored by decreases at 1654 cm^{-1}) were observed starting at 2.5 h and 8 h of incubation, and at longer times (>10 h) a steady increase in intensity at 1628 cm^{-1}, with a concomitant decrease in the intensity at 1654 cm^{-1}, was observed. The latter change reflects the conversion of soluble α-helical forms of insulin into β-structure-enriched fibrils. At 28 h of incubation the β-sheet composition was ~ 52 % as calculated from the FTIR spectrum.

These observations indicate the existence of stepwise changes in insulin secondary structure during the process of insulin fibrillation. To better account for these changes, we performed curve fitting of the FTIR spectra. Curve fitting of the native protein at 0 h of incubation shows the existence of a variety of secondary structural elements as shown in Table 2 and Figure 4. The same set of secondary structural components was observed for the 2.5 h spectrum. However, dramatic changes in secondary structure content were observed between 2.5 - 3.0 h of incubation (Figure 4, Table 2). Although it is very difficult to delineate between intra-molecular unfolding and the inter-molecular association from FTIR spectra, one thing that the fitting data clearly shows is the loss of most of the secondary structural elements belonging to the native monomer during this small interval of time. This is strong evidence for the formation of a partially unfolded intermediate of the insulin monomer before any fibrillation has taken place. At longer times of incubation the FTIR spectra are dominated by the contributions of β-structure (at 1628 cm^{-1}). Based on the results of dynamic light scattering (see below) we attribute the first transition, between 2.5 and 5 h to formation of a partially unfolded intermediate that rapidly associates to form soluble oligomers, and the second transition, from 7-11 h to formation of a second oligomeric intermediate, as well as concomitant fibril formation.

Circular Dichroism Spectra: Far-UV CD spectra have been used as a finger print region for the identification of various secondary structural elements. Far-UV CD spectra obtained for insulin at various times of incubation are shown in Figure 5. The CD spectrum measured for the sample before the beginning of incubation has double minima at 208 and 222 nm, which is characteristic of α-helical structure (the spectrum also shows evidence for β-sheet, hence the helical signature is not so distinct). Spectra obtained from samples incubated up to 2 hours do not exhibit any significant difference from the native monomer. However, after 3 hours of incubation the spectral shape starts to change. This finding supports the above mentioned

observations that major changes in insulin structure occur between 2 and 3 h, and well before any fibrillation takes place. The spectrum obtained at 6 hours shows more β-sheet than α-helical structure, with a single minimum observing at around 217 nm. After 8 hours of incubation the spectrum resembles that of predominant beta structure. Further incubation of insulin results only in an increase of beta content.

The analysis of CD data in a form of phase diagrams (or parametric dependencies) has been recently shown to represent a useful tool to elucidate fine details about structural changes occurring in insulin (*18;19*). Each linear leg of the phase diagram shows an all-or-none transition (*34-36*). A phase diagram for the above CD data was obtained by plotting ellipticity at 205 nm against 217 nm (Figure 5B). The data shows five straight line regions, corresponding to: 0-1.0; 1.0-4.0; 5.0-8.0; 8.0-13.0; 13.0-24.0 hrs. If each line represents a transition from one form to another, then the phase diagram analysis reveals the existence of at least 5 different transitions separating 6 different conformations during the insulin fibrillation. Whereas the initial two conformations can be attributed to changes within monomeric insulin in the early stages of aggregation, subsequent changes occurring after 5 h of incubation reflect transitions within different oligomeric conformations and ultimately fibrils. As with the other probes, the major transitions are around 5 and 12 h.

Dynamic light scattering: In order to determine if oligomeric intermediates were present during the incubation samples were taken as a function of time, centrifuged to remove any fibrillar material, and analyzed with dynamic light scattering. The monomer, and initial samples showed a single population of R_s = 1.0±0.1 nm (Mr = 5-6 kDa), corresponding to the monomer. After 2 h a small amount of a new component with R_s = 12.5±0.4nm appeared in addition to the monomer peak (Fig. 6). This oligomeric peak increased in population with increasing time of incubation, as the monomer peak correspondingly decreased. The monomer peak disappeared

after 8 h, whereas the oligomeric component reached a maximum population around 10 h and was still present at 25 h. The peak for the oligomeric species was quite broad, indicating the presence of a heterogeneous mixture of oligomers. Interestingly, in the 2 mg/ml insulin incubation, the size range of the oligomers was notably smaller, with some oligomers of ~ 5 nm radius. After 6 h the population of the oligomeric species increases dramatically, and the size distribution of the oligomers changes and becomes noticeably broader after 6 h, indicating a significant change in the nature of the species present starting around 6 h. In fact, based on the 2 mg/ml insulin data, it is likely that after 5 h a new, relatively low abundance, population of smaller oligomers is present, in addition to the larger ones.

DISCUSSION

The mechanistic details of the pathway that a protein follows from its monomeric state until it assembles into an ordered amyloid-like fibril have remained elusive because of the complex nature of the process. For example, α-synuclein, Aβ, and several other natively unfolded proteins transform into β-sheet rich fibrils rapidly after *gaining* a critical amount of ordered secondary structure [reviewed in (*6*)], whereas globular proteins undergo faster fibrillation upon *destabilization* of their secondary structure. In some cases, perturbing a sensitive balance of net charge of the protein (e. g. acylphosphatase (*37*), α-synuclein (*38-40*), or insulin) induces fibrillation. For insulin (as well as for many other proteins (*6*)) there is ample evidence favoring the existence of a partially folded intermediate on the fibrillation pathway. In our previous studies of insulin fibrillation we have generated a series of intermediate conformations by treatment with Gdn.HCl (*18*) or urea (*19*), and found them to be the species most prone to fibrillation - thus supporting the proposed mechanism that partially folded conformations are

critical for amyloidosis. In the present work we have obtained further evidence confirming that insulin also undergoes aggregation and fibrillation through a partially folded intermediate in the absence of denaturants.

An overall view of the details of insulin fibrillation is provided in Figure 7. In Figure 7A various biophysical changes taking place as a function of time have been normalized to unity. The calculated populations of two intermediate species on the fibrillation pathway starting with monomeric insulin are shown in Figure 7B. Intermediate I reaches a maximum concentration around 5 h of incubation, and intermediate II reaches a maximum concentration around 10-12 h. The intermediates are distinguishable by FTIR, CD and ANS binding, reflecting the significantly different underlying conformations. The intermediates also correspond to significant differences in the association state of insulin, as determined by dynamic light scattering. Examination of the time course of changes in the various probes all reveal the same critical times for significant changes in signal, namely around 2.5, 5, 8 and 12 h. Thus, it is clear that major changes in the aggregation process occur at these times. The simplest explanation is that these are transformations from one aggregation intermediate to another.

Whereas the fluorescence of ThT does not usually increase appreciably in the presence of partially folded intermediates or soluble oligomeric species, ANS fluorescence shows detectable changes in its properties (wavelength and intensity of maximal fluorescence) if partially folded intermediates are formed, and has been successfully used to monitor the process of fibril formation in other studies (*41-44*). Our ANS data reveal the presence of several conformational transitions within the initial stages of insulin fibrillation: the hydrophobic regions of insulin were found to become solvent exposed at 2.5 hrs. The saturation of blue shift of ANS fluorescence, λ^{ANS}_{max}, by 6 hrs indicates that the majority of protein molecules have undergone this change by that time. On the other hand, the saturation in the increase in ANS fluorescence intensity,

I^{ANS}_{max}, was approached much later, by 12 hrs, indicating the existence of some other structure-transforming processes that takes place between 6 and 12 hrs of incubation. The potential concentration effects of ANS in this behavior could be excluded as comparable results were obtained for different ratios of excess ANS over insulin (data not shown). The DLS data indicate that this involves a change in the nature of the oligomeric intermediate(s). The observed incongruity between the time courses of λ^{ANS}_{max} and I^{ANS}_{max} is also probably due to the fact that not only the fibrils but also the oligomeric intermediates are able to bind ANS. ATR-FTIR and far-UV CD data show that the appearance of the pre-fibrillar oligomers is accompanied by detectable changes in insulin secondary structure. Thus, the combined picture of insulin fibrillation shows a clear differentiation into several steps involving pre-fibrillation products. The first peaks at 5 hrs and another around 10-12 hrs, before transformation into the mature fibrils after 20 hrs of incubation. A critical look at Figure 7 also suggests the existence of an additional intermediate between 6-8 hrs, which is also consistent with the DLS data.

A major finding of this study, namely the partial unfolding of the insulin monomer before the beginning of fibrillation, is best indicated by the appearance of ANS-binding species at 2.5 hours of incubation, before any detectable fibrillation is observed. The ATR FTIR data supports this observation, showing the loss of the majority of secondary structural elements. Additional strong support of this idea comes from the H/D exchange mass spectroscopic data, which revealed that 10 originally buried and protected protons undergo slow H/D exchange at 2.5 hrs of incubation. In previous studies insulin has been found to have total of 15±2 protons accessible for the slow exchange (*45*), of which 4 have been traced to residues 14-17 of the A chain and 6 to residues 12-16 of the B chain. The remaining 5 protons were shown to be buried in the N-terminal hydrophobic region and are very inaccessible (*45*). Our analysis revealed the exchange of 10 protons at 2.5 hours. We assume that these 10 slow exchanging protons belong to the middle

regions of the A and B chains of the protein. The parent ion peak obtained under these conditions differed from the insulin monomer only by these 10 units confirming the monomeric state of insulin. These results favor the existence of a non-native conformation before the onset of any association, and it is likely that this conformation actually triggers the association of monomers into fibrils.

Thus, the present study suggests that the fibrillation of the monomeric insulin is a sequential process, where the structural transformation of the rigid native monomeric protein into a flexible partially folded conformation represents a very important early step in the pathway to fibrils. Although an environment conducive for fibrillation was used in the present study, we believe that a similar situation will exist in the absence of such conditions *in vivo*. The significantly lower concentrations of the intermediate species may be the reason for the normal absence of fibrillation in vivo. The data presented also shows that models for fibril structure, based on the three-dimensional structure of the insulin native state (*46-49*) are unlikely to be correct.

References

1. Kelly, J. W. (1998) The alternative conformations of amyloidogenic proteins and their multi-step assembly pathways, *Curr. Opin. Struct. Biol 8*, 101-106.

2. Bellotti, V., Mangione, P., and Stoppini, M. (1999) Biological activity and pathological implications of misfolded proteins, *Cell. Mol. Life Sci. 55*, 977-991.

3. Uversky, V. N., Gillespie, J. R., Talapatra, A., and Fink, A. L. (1999) Protein Deposits as the Molecular Basis of Amyloidosis: Part I. Systemic amyloidosis, *Med. Sci. Monitor 5*, 1001-1012.

4. Uversky, V. N., Gillespie, J. R., Talapatra, A., and Fink, A. L. (1999) Protein Deposits as the Molecular Basis of Amyloidosis: Part II. Localized amyloidosis and neurodegenerative disorders., *Med. Sci. Monitor 5*, 1238-1254.

5. Rochet, J. C. and Lansbury, P. T., Jr. (2000) Amyloid fibrillogenesis: themes and variations, *Curr. Opin. Struct. Biol. 10*, 60-68.

6. Uversky, V. N. and Fink, A. L. (2004) Conformational constraints for amyloid fibrillation: the importance of being unfolded, *Biochim. Biophys. Acta 1698*, 131-153.

7. Dobson, C. M. (1999) Protein misfolding, evolution and disease, *Trends Biochem. Sci. 24*, 329-332.

8. Dobson, C. M. (2001) Protein folding and its links with human disease, *Biochem. Soc. Symp.* 1-26.

9. Fandrich, M., Fletcher, M. A., and Dobson, C. M. (2001) Amyloid fibrils from muscle myoglobin - Even an ordinary globular protein can assume a rogue guise if conditions are right, *Nature 410*, 165-166.

10. Pertinhez, T. A., Bouchard, M., Tomlinson, E. J., Wain, R., Ferguson, S. J., Dobson, C. M., and Smith, L. J. (2001) Amyloid fibril formation by a helical cytochrome, *FEBS Lett. 495*, 184-186.

11. Burke, M. J. and Rougvie, M. A. (1972) Cross- protein structures. I. Insulin fibrils, *Biochemistry 11*, 2435-2439.

12. Waugh, D. F. (1946) A fibrous modification of insulin. I. The heat precipitate of insulin, *J. Am. Chem. Soc. 68*, 247-250.

13. Nielsen, L., Khurana, R., Coats, A., Frokjaer, S., Brange, J., Vyas, S., Uversky, V. N., and Fink, A. L. (2001) Effect of environmental factors on the kinetics of insulin fibril formation: elucidation of the molecular mechanism, *Biochemistry 40*, 6036-6046.

14. Nielsen, L., Frokjaer, S., Carpenter, J. F., and Brange, J. (2001) Studies of the structure of insulin fibrils by Fourier transform infrared (FTIR) spectroscopy and electron microscopy, *J. Pharm. Sci. 90*, 29-37.

15. Jimenez, J. L., Nettleton, E. J., Bouchard, M., Robinson, C. V., Dobson, C. M., and Saibil, H. R. (2002) The protofilament structure of insulin amyloid fibrils, *Proc. Natl. Acad. Sci U. S. A 99*, 9196-9201.

16. Dische, F. E., Wernstedt, C., Westermark, G. T., Westermark, P., Pepys, M. B., Rennie, J. A., Gilbey, S. G., and Watkins, P. J. (1988) Insulin as an amyloid-fibril protein at sites of repeated insulin injections in a diabetic patient, *Diabetologia 31*, 158-161.

17. Brange, J., Andersen, L., Laursen, E. D., Meyn, G., and Rasmussen, E. (1997) Toward understanding insulin fibrillation, *J. Pharm. Sci. 86*, 517-525.

18. Ahmad, A., Millett, I. S., Doniach, S., Uversky, V. N., and Fink, A. L. (2003) Partially folded intermediates in insulin fibrillation, *Biochemistry 42*, 11404-11416.

19. Ahmad, A., Millett, I. S., Doniach, S., Uversky, V. N., and Fink, A. L. (2004) Stimulation of insulin fibrillation by urea-induced intermediates, *J. Biol. Chem. 279*, 14999-15011.

20. Nielsen, L., Frokjaer, S., Brange, J., Uversky, V. N., and Fink, A. L. (2001) Probing the Mechanism of Insulin Fibril Formation with Insulin Mutants, *Biochemistry 40*, 8397-8409.

21. Naiki, H., Higuchi, K., Hosokawa, M., and Takeda, T. (1989) Fluorometric Determination of Amyloid Fibrils *in Vitro* Using the Fluorescent Dye, Thioflavin T, *Analytical Biochemistry 177*, 244-249.

22. LeVine, H., III (1993) Thioflavine T interaction with synthetic Alzheimer's disease beta-amyloid peptides: detection of amyloid aggregation in solution, *Protein Sci. 2*, 404-410.

23. Semisotnov, G. V., Rodionova, N. A., Kutyshenko, V. P., Ebert, B., Blanck, J., and Ptitsyn, O. B. (1987) Sequential mechanism of refolding of carbonic anhydrase b, *Febs Letters 224*, 9-13.

24. Semisotnov, G. V., Rodionova, N. A., Razgulyaev, O. I., Uversky, V. N., Gripas', A. F., and Gilmanshin, R. I. (1991) Study of the "molten globule" intermediate state in protein folding by a hydrophobic fluorescent probe., *Biopolymers 31*, 119-28.

25. Fink, A. L. (1999) ANS, in *The Encyclopedia of Molecular Biology* (T.E.Creighton, Ed.) pp 140-142, John Wiley & Sons, New York.

26. Stryer, L. (1965) The interaction of a naphthalene dye with apomyoglobin and apohemoglobin. A fluorescent probe for nonpolar sites., *J Mol Biol 13*, 482-95.

27. Buijs, J., Vera, C. C., Ayala, E., Steensma, E., Hakansson, P., and Oscarsson, S. (1999) Conformational stability of adsorbed insulin studied with mass spectrometry and hydrogen exchange [In Process Citation], *Anal. Chem. 71*, 3219-3225.

28. Ramanathan, R., Gross, M. L., Zielinski, W. L., and Layloff, T. P. (1997) Monitoring recombinant protein drugs: a study of insulin by H/D exchange and electrospray ionization mass spectrometry, *Anal. Chem. 69*, 5142-5145.

29. Seshadri, S., Khurana, R., and Fink, A. L. (1999) Fourier transform infrared spectroscopy in analysis of protein deposits, *Methods Enzymol. 309*, 559-576.

30. Fink, A. L., Seshadri, S., Khurana, R., and Oberg, K. A. (1999) Determination of Secondary Structure in Protein Aggregates Using Attenuated Total Reflectance (ATR) FTIR, in *Infrared Analysis of Peptides and Proteins* (B.R.Singh, Ed.) pp 132-144, Amer. Chemical Society, NY.

31. Wei, J., Xie, L., Lin, Y. Z., and Tsou, C. L. (1992) The pairing of the separated A and B chains of insulin and its derivatives, FTIR studies, *Biochim. Biophys. Acta 1120*, 69-74.

32. Wei, J. A., Lin, Y. Z., Zhou, J. M., and Tsou, C. L. (1991) FTIR studies of secondary structures of bovine insulin and its derivatives, *Biochim. Biophys. Acta 1080*, 29-33.

33. Vecchio, G., Bossi, A., Pasta, P., and Carrea, G. (1996) Fourier-transform infrared conformational study of bovine insulin in surfactant solutions, *Int. J. Pept. Protein Res. 48*, 113-117.

34. Bushmarina, N. A., Kuznetsova, I. M., Biktashev, A. G., Turoverov, K. K., and Uversky, V. N. (2001) Partially folded conformations in the folding pathway of bovine carbonic anhydrase II: a fluorescence spectroscopic analysis, *Chembiochem. 2*, 813-821.

35. Kuznetsova, I. M., Stepanenko, O. V., Turoverov, K. K., Zhu, L., Zhou, J. M., Fink, A. L., and Uversky, V. N. (2002) Unraveling multistate unfolding of rabbit muscle creatine kinase, *Biochim. Biophys. Acta 1596*, 138-155.

36. Kuznetsova, I. M., Turoverov, K. K., and Uversky, V. N. (2004) Use of the phase diagram method to analyze the protein unfolding-refolding reactions: fishing out the "invisible" intermediates, *J. Proteome. Res. 3*, 485-494.

37. Chiti, F., Webster, P., Taddei, N., Clark, A., Stefani, M., Ramponi, G., and Dobson, C. M. (1999) Designing conditions for in vitro formation of amyloid protofilaments and fibrils, *Proc. Natl. Acad. Sci U. S. A 96*, 3590-3594.

38. Uversky, V. N., Li, J., and Fink, A. L. (2001) Evidence for a partially folded intermediate in alpha-synuclein fibril formation, *J. Biol. Chem. 276*, 10737-10744.

39. Munishkina, L. A., Henriques, J., Uversky, V. N., and Fink, A. L. (2004) Role of protein-water interactions and electrostatics in alpha-synuclein fibril formation, *Biochemistry 43*, 3289-3300.

40. Uversky, V. N., Li, J., and Fink, A. L. (2001) Metal-triggered Structural Transformations, Aggregation, and Fibrillation of Human alpha -Synuclein. A possible molecular link between Parkinson's disease and heavy metal exposure, *J. Biol. Chem. 276*, 44284-44296.

41. Serio, T. R., Cashikar, A. G., Kowal, A. S., Sawicki, G. J., Moslehi, J. J., Serpell, L., Arnsdorf, M. F., and Lindquist, S. L. (2000) Nucleated conformational conversion and

the replication of conformational information by a prion determinant, *Science 289*, 1317-1321.

42. Souillac, P. O., Uversky, V. N., Millett, I. S., Khurana, R., Doniach, S., and Fink, A. L. (2002) Effect of association state and conformational stability on the kinetics of immunoglobulin light chain amyloid fibril formation at physiological pH, *J. Biol. Chem. 277*, 12657-12665.

43. Souillac, P. O., Uversky, V. N., Millett, I. S., Khurana, R., Doniach, S., and Fink, A. L. (2002) Elucidation of the molecular mechanism during the early events in immunoglobulin light chain amyloid fibrillation: Evidence for an off-pathway oligomer at acidic pH, *J. Biol. Chem. 277*, 12666-12669.

44. Souillac, P. O., Uversky, V. N., and Fink, A. L. (2003) Structural Transformations of Oligomeric Intermediates in the Fibrillation of the Immunoglobulin Light Chain LEN, *Biochemistry 42*, 8094-8104.

45. Tito, P., Nettleton, E. J., and Robinson, C. V. (2000) Dissecting the hydrogen exchange properties of insulin under amyloid fibril forming conditions: A site-specific investigation by mass spectrometry [In Process Citation], *J. Mol. Biol. 303*, 267-278.

46. Yao, Z. P., Zeng, Z. H., Li, H. M., Zhang, Y., Feng, Y. M., and Wang, D. C. (1999) Structure of an insulin dimer in an orthorhombic crystal: the structure analysis of a human insulin mutant (B9 Ser-->Glu), *Acta Crystallogr. D. Biol. Crystallogr. 55 (Pt 9)*, 1524-1532.

47. Shoelson, S. E., Lu, Z. X., Parlautan, L., Lynch, C. S., and Weiss, M. A. (1992) Mutations at the dimer, hexamer, and receptor-binding surfaces of insulin independently affect insulin-insulin and insulin-receptor interactions, *Biochemistry 31*, 1757-1767.

48. Brange, J., Dodson, G. G., Edwards, D. J., Holden, P. H., and Whittingham, J. L. (1997) A model of insulin fibrils derived from the x-ray crystal structure of a monomeric insulin (despentapeptide insulin), *Proteins 27*, 507-516.

49. Whittingham, J. L., Scott, D. J., Chance, K., Wilson, A., Finch, J., Brange, J., and Guy, D. G. (2002) Insulin at pH 2: structural analysis of the conditions promoting insulin fibre formation, *J. Mol. Biol. 318*, 479-490.

Table I. H/D exchange mass spectrometry of insulin. Aliquots obtained from different time intervals during the incubation of monomeric insulin were diluted 100 times with the required D_2O concentration and immediately injected into the capillary of the mass spectrometer.

H/D exchange for monomeric insulin		
D_2O %	**Hrs of incubation in D_2O**	**# of protons exchanged**
5 %	0 6 12 24	- - - -
10 %	0 6 12 24	- - 20 20
60 %	0 6 12	40 50 50
H/D exchange for aliquots from 4 mg/mL insulin incubated at 37 °C with		

continuous shaking			
D_2O %	**Hrs of incubation at 37 °C of aliquots**	**Hrs of incubation in D_2O**	**# of protons exchanged**
5 %	0 - 2.5	0	-
10 %	0 - 2.5	0	-
60 %	0 0.5 1.5 2.0 2.5	0 0 0 0 0	40 40 40 40 50

Table II. Secondary structure elements from FTIR analysis of insulin as a function of time of incubation. The wavenumbers (cm^{-1}) of the constituent secondary structural elements at various time intervals during its incubation for fibrillation are shown. Band components were obtained from curve fits of amide I spectra (see text for details).

0 hrs	**2.5 hrs**	**3.0 hrs**	**28.0 hrs**
cm^{-1}	**cm^{-1}**	**cm^{-1}**	**cm^{-1}**
1693.4	1694.5		1687.7
	1690.1	1689.1	
	1684.1		
1678	1675.8		1676.7
1665	1664.7	1669	1665.5
1654	1654.6	1653	
1644.2	1643.9		
1639	1638.7		1638.1
1633.3	1633.3		
1625	1624.7	1627.6	1626.9
1618			

	1614.4	1613	1613.9
1610			1606.3
1604	1603.50	1602.60	

Figure Legends

Figure 1. Fibrillogenesis of insulin as detected by changes in ThT fluorescence. Insulin 4 mg/mL (filled circles) and 2 mg/mL (open circles) in 20% acetic acid was incubated at 37 °C with continuous agitation, and aliquots were taken every 30 min, and assayed with ThT. Analysis of the kinetics gives a lag time of 11 h and 5 h for 2 and 4 mg/mL insulin, respectively.

Figure 2. Structural changes accompanying fibrillation of insulin as detected by ANS fluorescence. Aliquots (5 mL) of the incubation mixture of monomeric insulin were added to 3 mM ANS and the spectra recorded immediately. Open circles depict changes in λ_{max} of the ANS emission and solid circles represent the changes in the intensity at the maximum emission wavelength.

Figure 3 Changes accompanying the process of insulin fibrillation as detected by ATR-FTIR. Panel A: Aliquots (40 mL) from incubation of monomeric insulin at 37 °C were spread on a Ge crystal to form a thin hydrated film prior to collecting FTIR spectra. The numbers represent the time of incubation in hours. The figure shows the conversion of the predominant native helical peak at 1654 cm^{-1} and 0 hrs into a β-sheet-rich peak at 1628 cm^{-1} starting from 3 hours. Panel B:

Changes in absorbance at 1628 cm^{-1} (solid circles) and 1655 cm^{-1} (open circles) as a function of incubation time.

Figure 4. Changes in the secondary structure composition of insulin during fibrillation from FTIR spectra. Curve-fitting was used to identify the constituent secondary structure components (see methods section) (see also table II). Panel A: 0 h, panel B: 2.5 h, panel C: 3.0 h, panel D: 28.0 h.

Figure 5 Structural changes accompanying the process of insulin fibrillation as detected by far-UV CD. Panel A shows the CD spectra starting from the native monomer. At 0 h incubation, insulin exhibits a spectrum characteristic of an α-helical protein. As the time of incubation increases the negative ellipticity at 217 nm increases progressively, indicating conversion into a conformation enriched in β-sheet. Panel B shows the CD phase diagram indicating multiple transitions. The graph was obtained by plotting the ellipticity at 205 and 217 nm. The numbers in the plot indicate the incubation time.

Figure 6. *The mechanistic details of insulin fibrillation Panel A,* fractional changes in various parameters, filled *circles*; Changes in wavelength max of ANS emission, *open triangles*; ThT fluorescence, *open circles*; ANS fluorescence intensity, *solid triangles*; First transition in IR absorbance at 1628 cm-1, *open inverted triangles;* Second transition in IR absorbance at 1628 cm-1 *Panel B,* shows a population of each specie as a function of time. Dotted line was obtained by subtracting ThT changes from either ANS wavelength or IR first transition. Dashed line by subtracting ANS Florescence Intensity from either ANS wavelength max or IR first transition.

Solid line from ANS And ThT fluorescence. Dash-dot-dot from ThT fluorescence from Second IR transition.

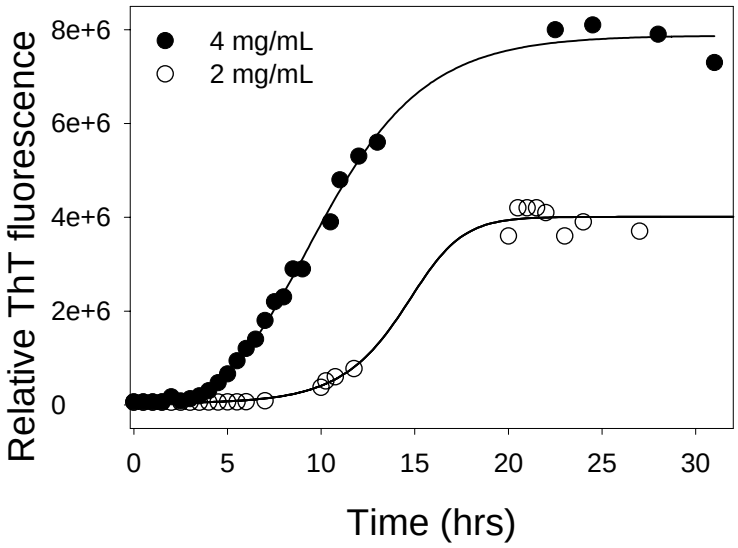

Figure 1

Ahmad et al.

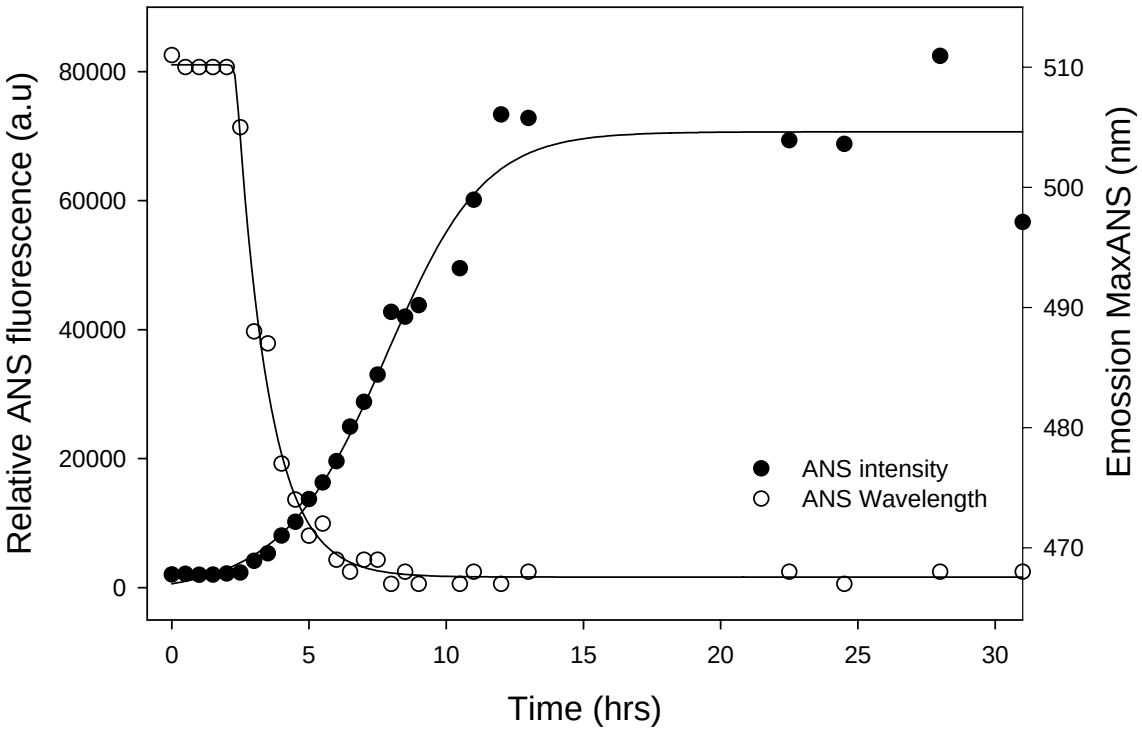
Relative ANS fluorescence (a.u)
80000
60000
40000
20000
0
0
5
10
15
20
25
30
Time (hrs)
510
500
490
480
470
Emossion MaxANS (nm)
ANS intensity
ANS Wavelength

Figure 2

Ahmad et al.

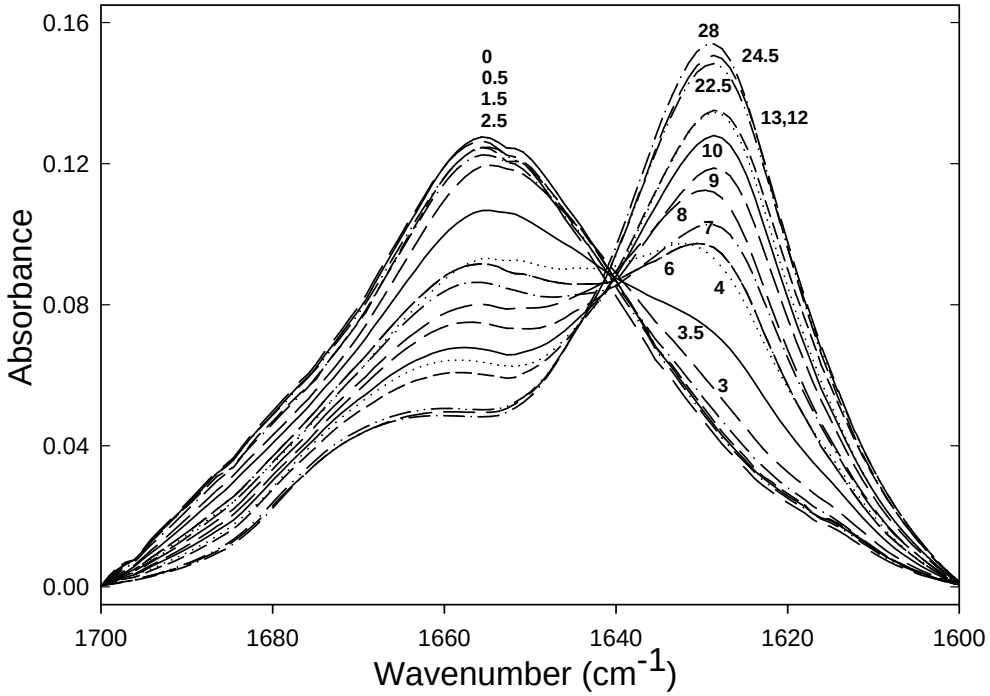
0.16
0.12
0.08
0.04
0.00
Absorbance
1700
1680
1660
1640
1620
1600
Wavenumber (cm-1)
0
0.5
1.5
2.5
28
24.5
22.5
13,12
10
9
8
7
6
4
3.5
3

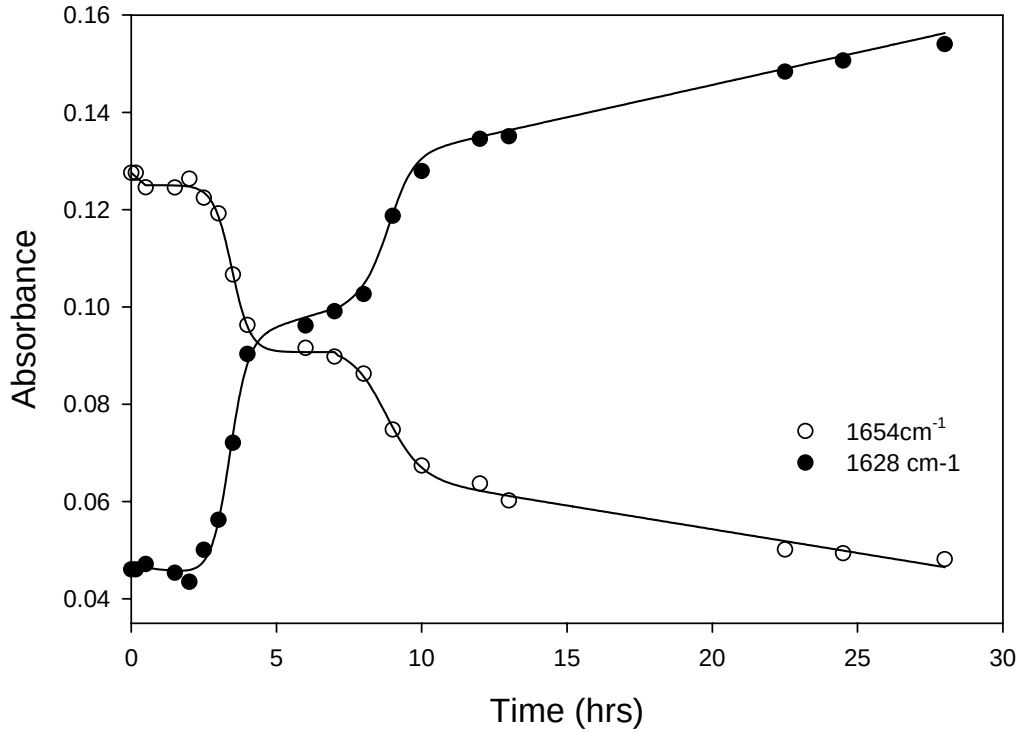
0.16
0.14
0.12
0.10
0.08
0.06
0.04
Absorbance
0
5
10
15
20
25
30
Time (hrs)
1654cm-1
1628 cm-1

Figure 3

Ahmad et al.

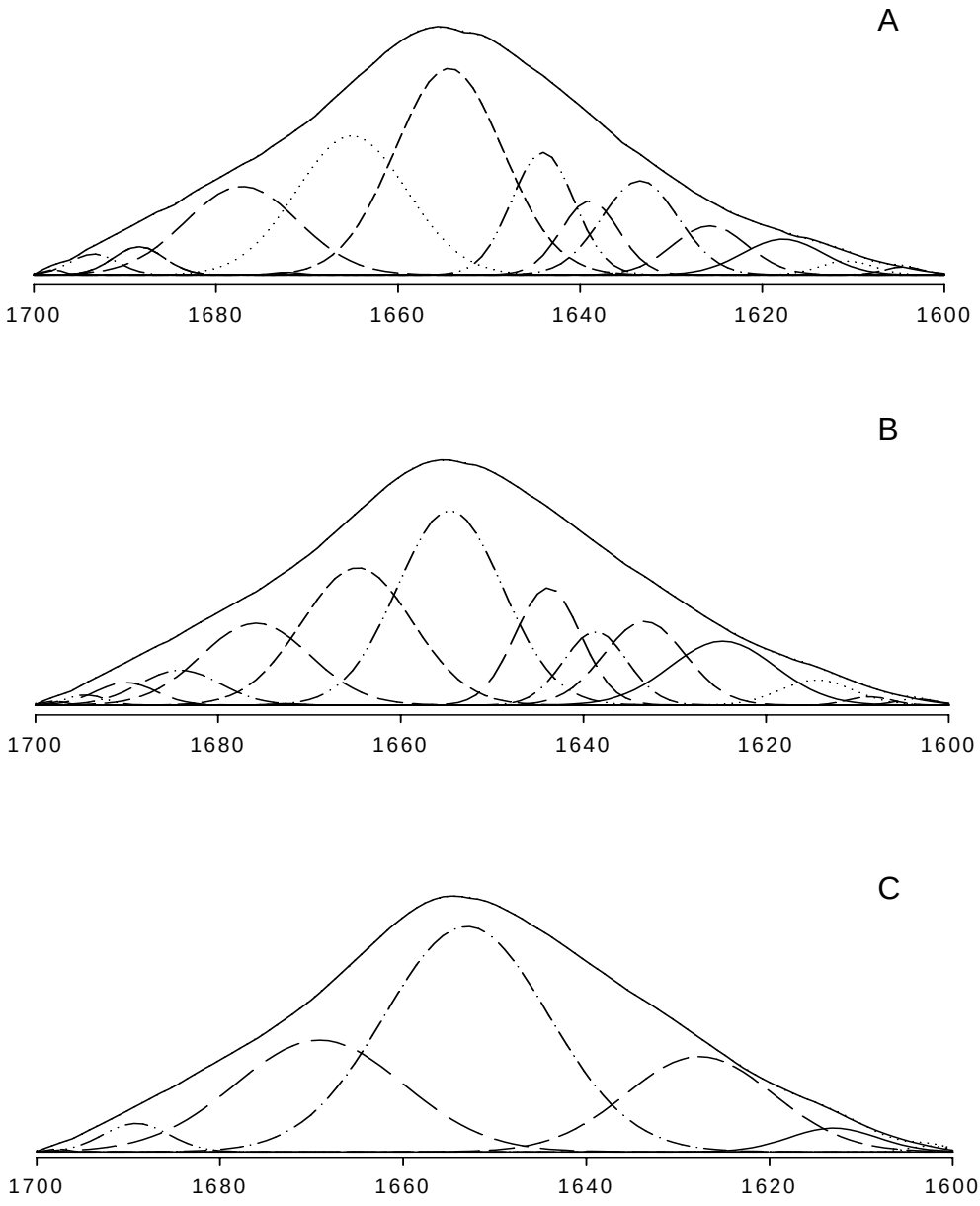
A
1700
1680
1660
1640
1620
1600
B
1700
1680
1660
1640
1620
1600
C
1700
1680
1660
1640
1620
1600

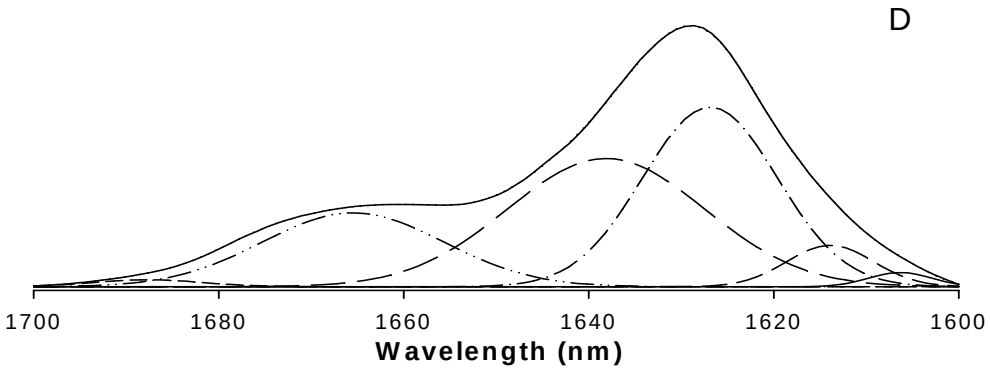
D
1700
1680
1660
1640
1620
1600
Wavelength (nm)

Figure 4

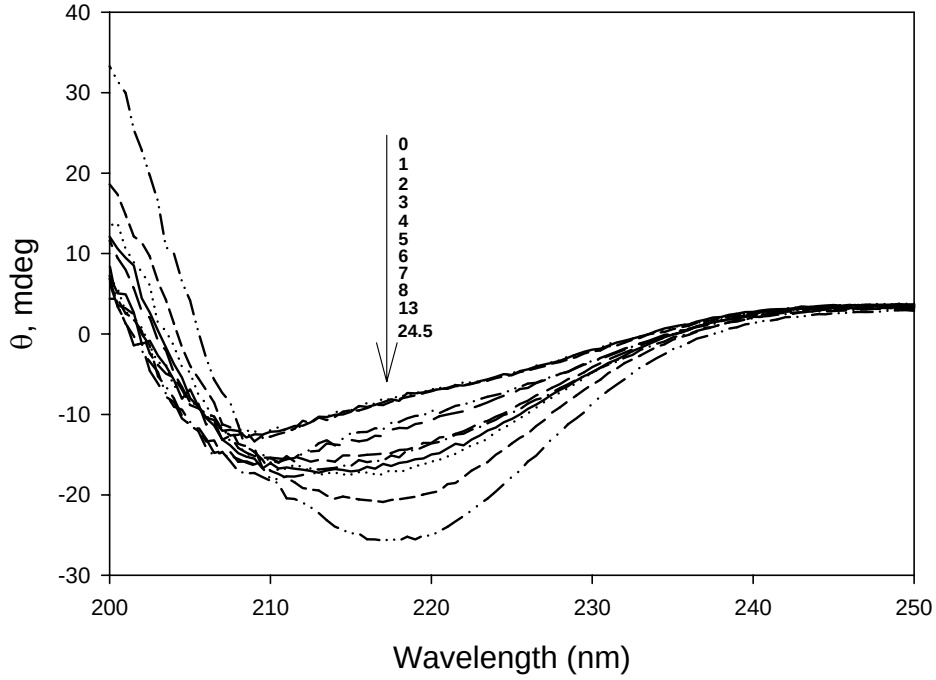
40
30
20
10
0
-10
-20
-30
θ, mdeg
0
1
2
3
4
5
6
7
8
13
24.5
200
210
220
230
240
250
Wavelength (nm)

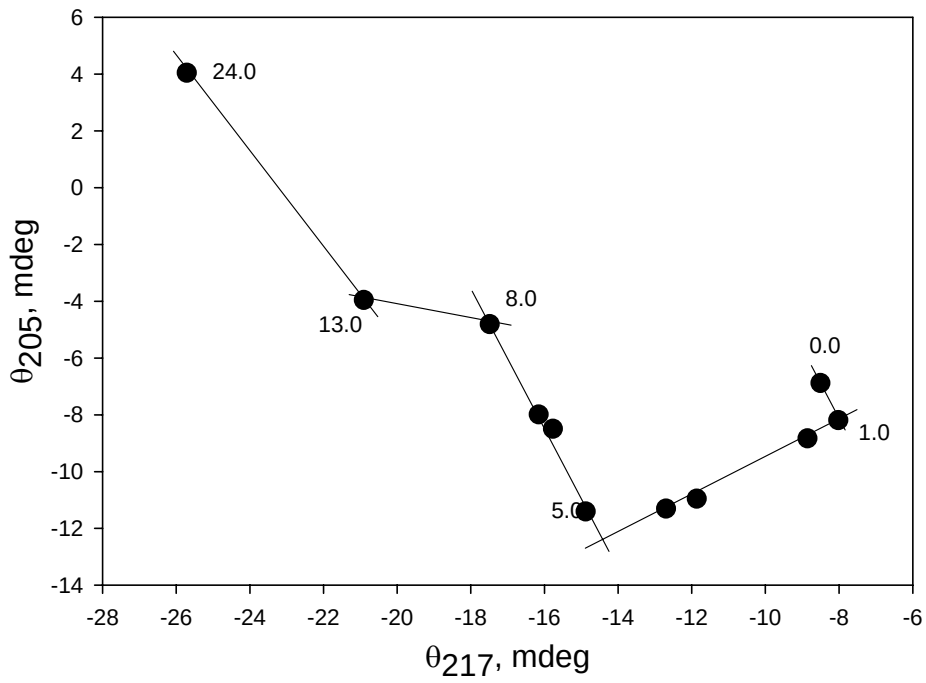

Figure 5

Ahmad et al.

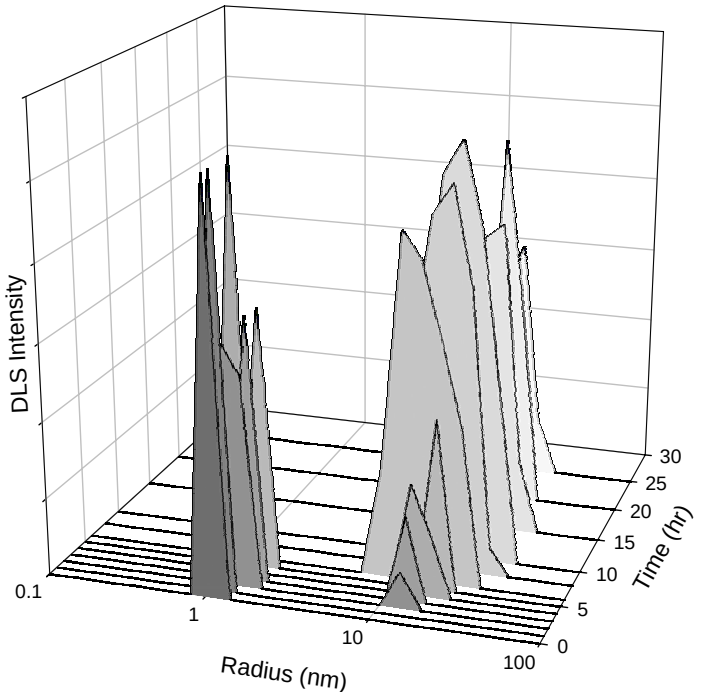

Figure 6

Ahmad et al.

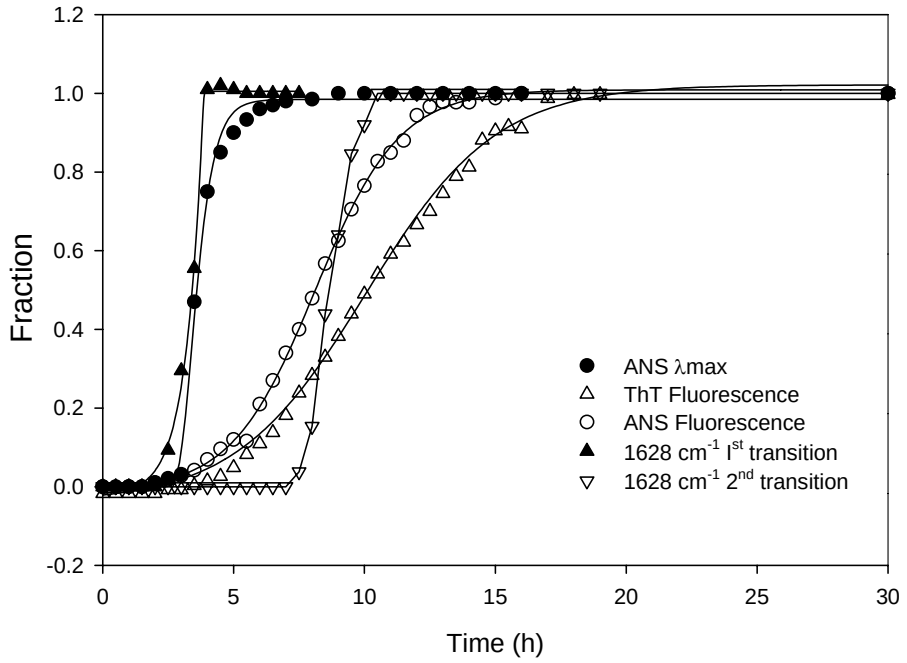

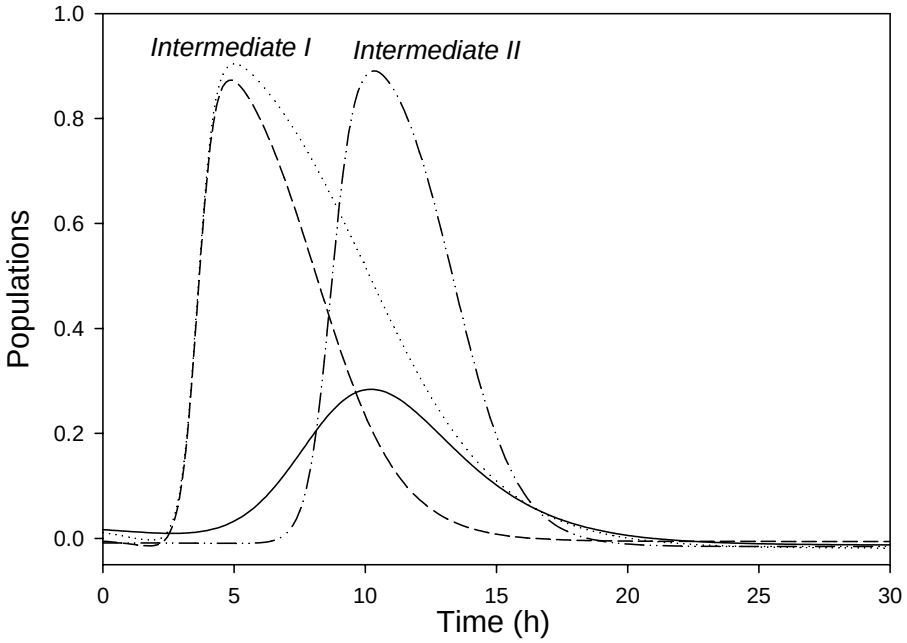

Figure 7
Ahmad et al.